Magnetic excitations in amorphous isotropic ferromagnets

H. A. Mook
Solid State Division, Oak Ridge National Laboratory, Oak Ridge, Tennessee 37830

J. W. Lynn
Department of Physics, University of Maryland, College Park, Maryland 20742
and National Measurement Laboratory, National Bureau of Standards, Washington, D.C. 20234
(Received 21 June 1983; revised manuscript received 28 November 1983)

Neutron-scattering techniques have been used to investigate the magnetic excitations in the structurally amorphous ideal isotropic ferromagnet ($T_c = 513$ K) $Fe_{40}Ni_{40}P_{14}B_6$. Small-angle inelastic-scattering measurements were taken with a triple-axis spectrometer to determine the temperature dependence of the spin-wave dispersion relation at long wavelengths. Most of the measurements, however, were concentrated in the momentum region near the first peak ($Q_0 = 3.1$ Å^{-1}) in the static structure factor, and were made at 295 and 17 K with a pulsed polarized-beam time-of-flight spectrometer that uses the cross-correlation technique of data collection to obtain a high signal-to-noise ratio. It is found that there is a "cone" of scattering as a function of energy with its apex at Q_0, in general agreement with the powder-averaged model proposed by Shirane *et al.* However, not all of the features of the data can be explained by this model; in particular at Q_0 there is a broad distribution of scattering as a function of energy with a maximum at $E \sim 12$ meV. Time-of-flight results are also presented for a single crystal and a powdered crystalline material in order to gain a better understanding of the corrections needed to obtain accurate data, and to establish that the instrument performs properly. The advantages as well as the limitations of this polarized-beam technique are discussed.

INTRODUCTION

There is increasing interest in understanding the spin dynamics of structurally amorphous materials since this can give us direct information important to the general behavior of randomized systems. In this paper we explore the nature of the magnetic excitations in the structurally amorphous isotropic ferromagnet $Fe_{40}Ni_{40}P_{14}B_6$ (Metglas®). Such materials are locally isotropic, and hence for length scales which are long compared to atomic dimensions, the structural disorder can be ignored and conventional spin-wave theory should adequately describe the spin dynamics. Indeed, well-defined spin waves are observed at long wavelengths, as they have been in a large number of other amorphous magnetic systems.[1,2] Such small-wave-vector measurements are important for understanding the overall magnetic behavior of those systems, but generally yield little direct information regarding the effects of the disorder on the spin dynamics. In order to observe most clearly the effects of disorder on the system, inelastic-scattering measurements need to be made at larger wave vectors where the dynamics are sampled on a length scale where the disorder is important. The first measurements of this type were made by Mook, Wakabayashi, and Pan[3] on Co_4P, and Mook and Tsuei[4,5] on $Fe_{75}P_{15}C_{10}$. The measurements on Co_4P were rather primitive because of the neutron absorption and high incoherent scattering associated with Co, and the difficulty of obtaining high-intensity polarized neutron beams necessary for the experiment, but the results established that magnetic excitations could be observed near the first peak in the static structure factor $S(Q)$ for the material. Details of the structure of the scattering were not obtained, except for the fact that the magnetic excitations reached a minimum in energy where a maximum is found in $S(Q)$. It was suggested at that time that these low-lying excitations might be similar in concept to the roton excitations in ^{4}He, and sum rules were utilized to make an analogy between the two cases. In retrospect, it is probably unwise to consider this connection too closely, although there is nothing incorrect, in principle, in utilizing the sum rules; the rotons in ^{4}He are simply that part of the phonon spectra that falls near the first peak in the static structure factor $S(Q)$ for superfluid ^{4}He. Thus one might call magnetic excitations near the first peak in $S(Q)$ of an amorphous material magnetic rotons. However, it is now clear that the shapes of the two types of excitations are quite different, the low-temperature rotons for ^{4}He being very sharp in energy, while the magnetic excitations for a metallic glass are spread over a rather large energy range. A better approach to understanding excitations in amorphous systems probably will stem from modeling the disorder, although to date only rather crude information has been obtained in this manner.

Considerably better measurements[4,5] were made on a sample of $Fe_{75}P_{15}C_{10}$ for several reasons. First, the incoherent nuclear cross section for iron is smaller than that for cobalt, and the energetics of the magnetic system are considerably reduced so that the excitations occur over a region of energy which is experimentally more favorable. Furthermore, ^{57}Fe polarizer-monochromator crystals had become available so that the incident polarized beam was

considerably higher in flux. Polarized-beam measurements are essential in these noncrystalline systems to distinguish the magnetic scattering at large Q from nuclear cross sections such as those originating from lattice vibrations and the static structure. A contour map of the magnetic inelastic scattering was presented for $Fe_{75}P_{15}C_{10}$ with details of the magnetic excitations, and the measurements resembled the computer-generated results of Alben.[6] However, both experimental errors and computer-termination errors prevented quantitative comparisons.

The present paper presents new measurements we have made on a large sample of $Fe_{40}Ni_{40}P_{14}B_6$. This material is the best-known isotropic ferromagnet, a property which has led to a number of commercial applications.[7] The long-wavelength excitations are conventional spin waves as we demonstrate below. The central attention, however, will be focussed on the nature of the scattering around the first peak in the structure factor. We first discuss the polarized-beam time-of-flight technique which was used in obtaining data in this Q range, emphasizing both the advantages and disadvantages of this technique. We will then present some test results of the spectrometer along with the data for the amorphous material. Finally, we discuss these results and compare them with other systems which have been studied as well as with model calculations.

EXPERIMENTAL TECHNIQUES

Since the time that the measurements were made on $Fe_{75}P_{15}C_{10}$, two additional polarized-neutron—scattering experiments have been made on amorphous ferromagnets near the first peak in $S(Q)$ using the triple-axis technique. The first of these is by Shirane *et al.*[8] and the second is by Paul *et al.*[9] Both sets of authors have discussed difficulties in using the partial-polarization technique as we use it, with Shirane *et al.*[8] paying particular attention to the difficulties with resolution effects in the energy range near zero energy transfer. It is thus desirable to discuss the neutron pulsed-polarization technique that is used in the present experiments, and to obtain measurements on model systems where the results are established. The spectrometer is located at the High-Flux Isotope Reactor at Oak Ridge National Laboratory, and has already been discussed in detail in Ref. 4. It utilizes a high-speed spin-flip device for good time-of-flight resolution and the cross correlation technique of data accumulation for a high signal-to-noise ratio.

The important feature of the polarized-beam technique is that unwanted contributions to the scattering intensity cancel. Thus in the ideal situation there is no contribution from nuclear cross sections such as from lattice vibrations, elastic structural scattering, incoherent scattering, etc. However, if there is appreciable scattering (depletion) of the incident beam, which is polarization dependent, then there will be a contribution from the spin-independent nuclear cross section which will not cancel exactly. This contribution will be observed in both the time-of-flight and triple-axis techniques. This "depolarization" effect in fact is found to be significant for measurements on both powders and amorphous materials. We will return to this point later.

One of the features of the present technique is that for neutron energy gain $S^{-+}(Q,E)$ will be the nonzero cross section, where we have used the notation of Ref. 8. This gives a negative contribution, whereas for energy loss $S^{+-}(Q,E)$ will be nonzero and the contribution will be positive. This causes no difficulty except[10] near $E=0$ where their subtraction causes a cancellation in the scattered intensity. This point has been carefully discussed in Refs. 8 and 9, and it is clear that the cross section of interest cannot be measured in the region near $E=0$ where the spectrometer resolution convolutes S^{+-} and S^{-+}.

SPECTROMETER TESTS

Before presenting the results on the Metglas sample we would like to present measurements on known systems so that the operation of the spectrometer can be ascertained. $Ho_{0.88}Tb_{0.12}Fe_2$ has the desirable property that it is a ferrimagnet and easily saturated magnetically at room temperature. In addition, intense magnetic inelastic scattering originates from a spin-wave mode at about 7 meV which has little dispersion near the zone boundary.[11] A 0.5-cm^3 single crystal of this material was mounted at the sample position. The results near the zone boundary are shown in Fig. 1. These data were obtained in a 12-h run using an incident energy of 37.0 meV. Note that the energy-gain intensity is negative, the energy-loss intensity is positive, and the statistical accuracy is very good. Clearly the spectrometer operates properly, yielding accurate results in a relatively short time. In this case sufficient resolution was used that the excitations for neutron energy gain and loss are well separated and problems with cancellation of the intensity near $E=0$ do not arise. It is thus clear that accurate measurements are possible for energy transfers which are outside the range of the spectrometer energy resolution around $E=0$.

The measurements made in Refs. 8 and 9 substantiated earlier results that there are low-energy magnetic excitations in amorphous magnets in the region near the first

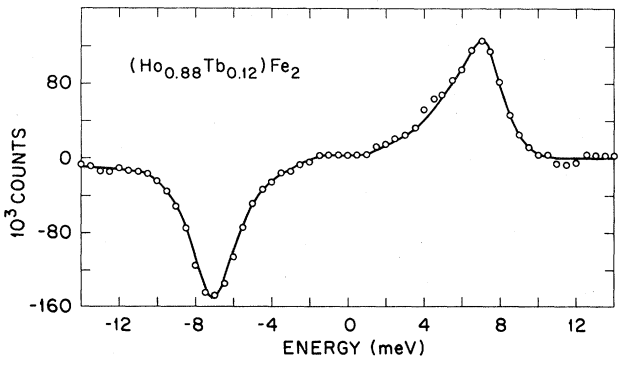

FIG. 1. Observed inelastic magnetic scattering obtained from the cross-correlation polarized-beam time-of-flight spectrometer for (TbHo)Fe_2. The intensity is proportional to $S^{+-}(Q,E)-S^{-+}(Q,E)$. For magnon creation ($E>0$), $S^{-+}=0$, and only S^{+-} contributes, whereas for magnon destruction ($E<0$), $S^{+-}=0$.

peak in the structure factor. Both sets of measurements were compared to results expected for a polycrystalline material, which has a different type of scattering pattern than had been reported for amorphous materials as measured by the present time-of-flight technique. Shirane *et al.*[8] calculated the scattering expected from a polycrystal, and it is thus worthwhile to determine if we can make an accurate measurement on a polycrystal. This is not especially easy since depolarization turns out to be a significant problem, but we found that a commercially available MnNiZn ferrite could be measured. This material has several advantages; it can be readily saturated at room temperature in moderate fields with relatively small depolarization effects, the magnetic moment is high, and the lattice constant is large so that phonon scattering is minimized in the vicinity of the first reflection. The incident energy was chosen to be 26.21 meV, with a pseudorandom sequence 683 units long and a 5-μsec time channel. Data were obtained in six banks of detectors at angles between 11.5° and 21.2°. The lattice constant of the material is 8.33 Å so that the (111) Bragg peak occurs at 1.31 Å^{-1}. Data were collected in time-of-flight channels for each detector and then cross-correlated to obtain the scattered intensity as a function of time of flight. The data in different detectors were corrected for detector efficiency by comparison with a vanadium standard; the variation with energy of the efficiency of each individual detector is very small over the region of interest, and no corrections were made for this. The results were then converted to equally spaced energy channels and multiplied by $(K_0/K')^4$ to give $S(Q,E)$. The room background was also subtracted in the process, which is easy to evaluate since many channels are available for background assessment in each detector. In addition, the magnetic scattering is directly proportional to the square of the magnetic form factor $f(Q)$. We assumed that the form factor for this material could be approximated sufficiently well by the measured form factor of metallic iron, and divided the data at each Q by $f(Q)^2$ for iron. This is a small correction, and certainly does not affect the results in any qualitative way. The resulting $S(Q,E)$ can then be compared with theory.

An alternative quantity which can be compared with theory is the dissipative part of the dynamic susceptibility $\chi(Q,E)$ which is related to the scattering function via the thermal population factor (apart from multiplicative factors),[12]

$$S(Q,E)=\chi(Q,E)\frac{\exp(E/kT)}{\exp(E/kT)-1}\ , \tag{1}$$

where χ denotes the imaginary part of the susceptibility. For describing the low-temperature magnetic properties, the susceptibility is generally preferred since it is essentially temperature independent, whereas the measured $S(Q,E)$ will be strongly temperature dependent even though the magnetic response of the system does not change appreciably. Usually it is a matter of taste as to which function is used, but difficulties can be encountered for systems which have a broad distribution of scattering as a function of energy. If there can be any ambiguity it is advisable to study both functions, and therefore we will present our experimental results in terms of both quantities.

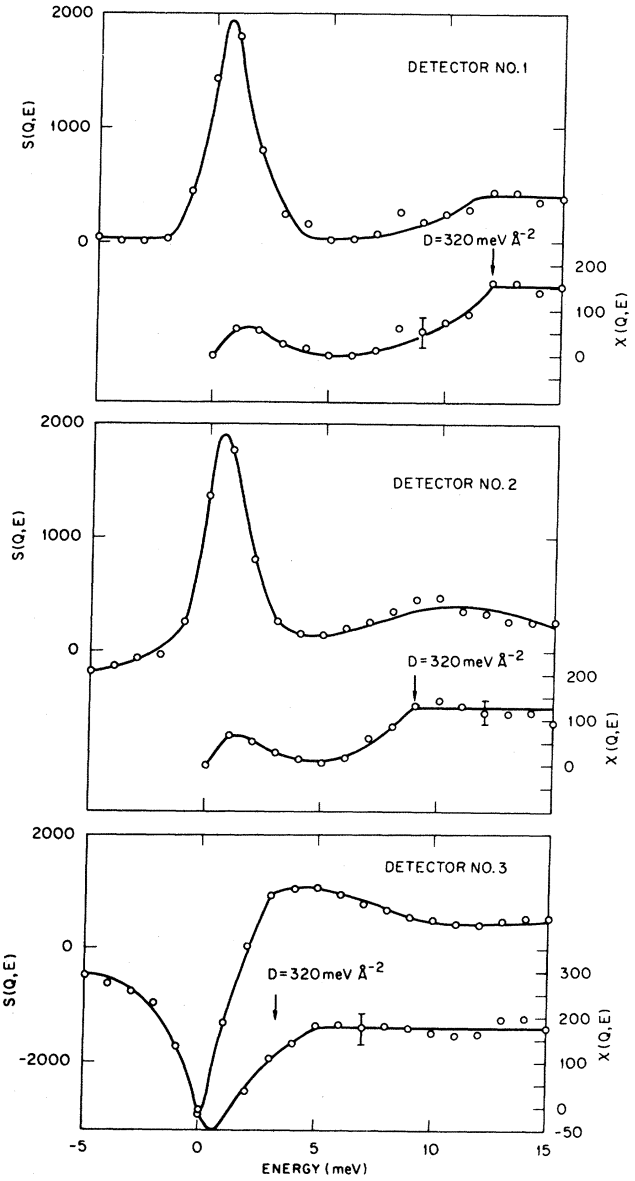

FIG. 2. Observed scattering from the polycrystal specimen for several detectors. The susceptibility [defined by Eq. (1)] is also shown. Note that the intensity scales are different for $S(Q,E)$ and $\chi(Q,E)$. The solid curves are simply a guide to the eye.

Figure 2 shows results from three of the detector banks for the powder measurement. Time-of-flight scans are at constant scattering angles so that the scan trajectory in (E,Q) space is a parabola. The scan trajectories are shown in Fig. 3 for each detector bank. Since the data must be multiplied by $(K_0/K')^4$, the counting errors become larger at larger energy transfers for neutron energy loss. All our results to be presented for the contour plots were taken from the neutron—energy-loss data, for which the neutrons slow down after scattering, and better time resolution is obtained. The time channels become closer together in energy as the neutron loses more energy, so more channels are available for conversion to constant energy channels. However, since all channels contain room back-

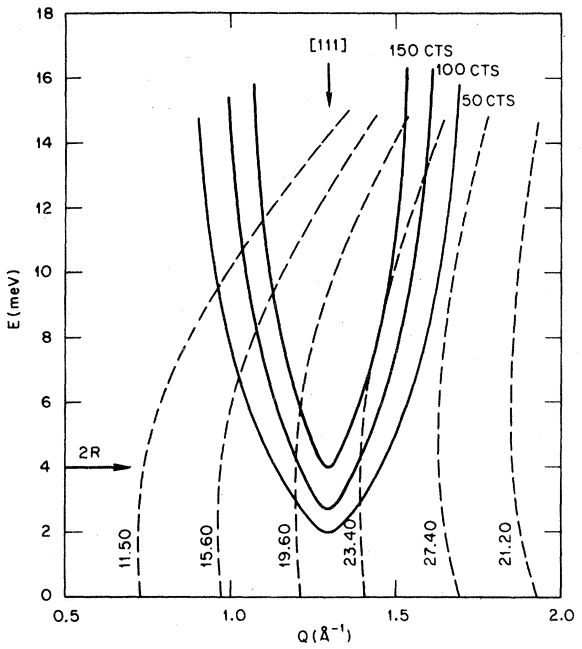

FIG. 3. Smoothed contours (solid curves) of the susceptibility obtained for the polycrystal. The dashed lines show the trajectories in (Q,E) space for each bank of detectors. Within experimental error the intensity is constant inside the curve labeled 150. The arrow labeled "$2R$" signifies twice the FWHM energy resolution; below this value the data are strongly affected by resolution effects.

ground as well as useful signals, the net result is still that statistical errors increase at higher-energy transfers. (The data collection is analogous to the case where a triple-axis spectrometer is used with fixed incident energy, and the analyzer moved in equal steps.) Generally useful data can be obtained for an energy transfer somewhat larger than one-half of the incoming energy, depending on the difficulty of the measurement.

We find that in the pattern for the polycrystal there is a peak in each detector at zero energy transfer. These peaks are not observed in single-crystal samples such as in Fig. 1, but occur in powders and amorphous materials and stem from the polarization effect discussed in Ref. 8.

The susceptibility $\chi(Q,E)$ is also shown in Fig. 2. $\chi(Q,E)$ for detector 1 gradually increases with increasing energy transfer up to $E\sim 12$ meV, and then is roughly constant at about 150 counts at higher energies. Detector 2 shows a similar pattern with a peak near $E=0$ and a constant intensity above about 9 meV. Detector 3, whose trajectory passes close to the (111) powder-diffraction line, shows a different type of pattern. In the absence of the polarization and resolution effects, the cancellation between $S^{-+}(Q,E)$ and $S^{+-}(Q,E)$ should produce a null result at $E=0$. However, the different transmission of the sample for the two polarization states, and the fact that the spectrometer resolution is slightly energy dependent, results in a shift of the zero crossover to positive energy. Thus, near the Bragg point we have an effect that is even worse than the straight cancellation of intensities, in that the negative scattering prevails and extends into the neutron—energy-loss region. Note that the resulting experimental (uncorrected) $\chi(Q,E)$ is in fact negative near $E=0$ and does not become positive until about 2 meV. A contour map for $\chi(Q,E)$ is shown in Fig. 3, and we see we have a pattern that resembles a "cone." The model calculation[8] yields a "cone" of scattering (actually a paraboloid of revolution if the dispersion relation is purely quadratic). Within experimental uncertainties the measured cone has a nearly constant intensity of about 150 counts, and the cone sides are consistent with a spin-wave-stiffness constant D of about 320 meV Å^{-2}. This value for D is quite reasonable, being between the ranges of D found for the spin waves in Fe_3O_4 and $MnFe_2O_4$ in Refs. 13 and 14. In the results for detector 3, we see that the constant intensity level is not reached at an energy corresponding to a D value of 320 meV Å^{-2}. We believe this is due to resolution effects which distort the data near $E=0$. These resolution effects should not be important in regions sufficiently far from $E=0$ where the cancellation and polarization effects are small. Note that for the data of detectors 1 and 2 the polarization peaks do not extend beyond about 4 meV, which is two resolution widths full width at half maximum (FWHM) removed from $E=0$. We thus expect our results to be good for energies above 4 meV and, indeed, the data for detector 3 reach the constant level at 5 meV. We remark that $S(Q,E)$ for a given Q is not expected to be constant in the cone, but that $\chi(Q,E)$ is. In fact, $S(Q,E)$ for the cone will be different depending on the temperature of the measurement.

Within the limitations of this technique our measurement of the cone of scattering expected for a polycrystal is quite successful, and, in fact, a reasonable estimate of the spin-wave-stiffness coefficient could be obtained for ferromagnetic and ferrimagnetic materials for which single-crystal specimens were not available. Thus we conclude that the spectrometer works well for both single crystals and powders, but it is clear that care must be exercised in interpreting the powder data.

MEASUREMENTS ON AMORPHOUS $Fe_{40}Ni_{40}P_{14}B_6$

Since the magnetic excitations in amorphous materials are distributed over a large region of momentum and energy, measurements are difficult and it is important to get as favorable an experimental situation as possible. The system we have chosen to study is $Fe_{40}Ni_{40}P_{14}B_6$ (Metglas), which is a transition-metal—metalloid glass produced by rapid quenching from the melt.[7] The small coercivity and large permeability of this material have led to a number of commercial applications, and the size of the sample is only limited by pragmatic considerations. For the present purposes the "soft" magnetic properties mean that this system is an ideal isotropic ferromagnet. Thus at long wavelengths the spin-wave dispersion relation will be given by conventional spin-wave (SW) theory,[15]

$$E_{\mathrm{SW}}=D(T)q^2\,, \tag{2}$$

where any gap in the spectrum is completely negligible. The long-wavelength spin dynamics were investigated at the National Bureau of Standards research reactor using a

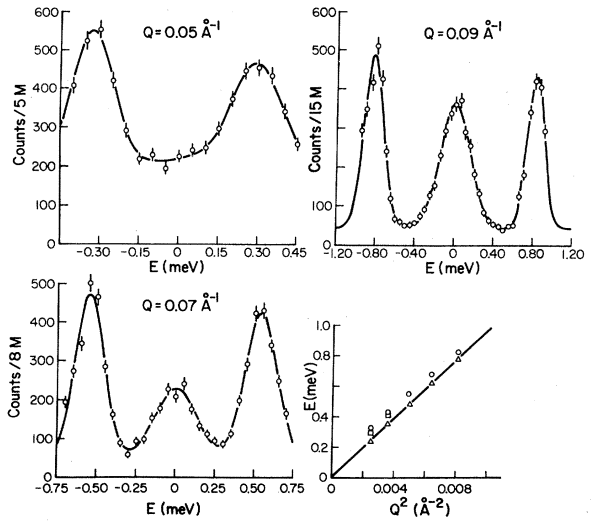

FIG. 4. Small-wave-vector inelastic scattering for $Fe_{40}Ni_{40}P_{14}B_6$ observed at room temperature. The magnons are observed in neutron energy gain ($E<0$) and loss ($E>0$). The elastic peak is nonmagnetic scattering which originates from the sample and furnace. The dispersion relation for energy gain (open circles) and loss (open squares) is seen to be quadratic to a very good approximation after correction (open triangles) for the instrumental resolution.

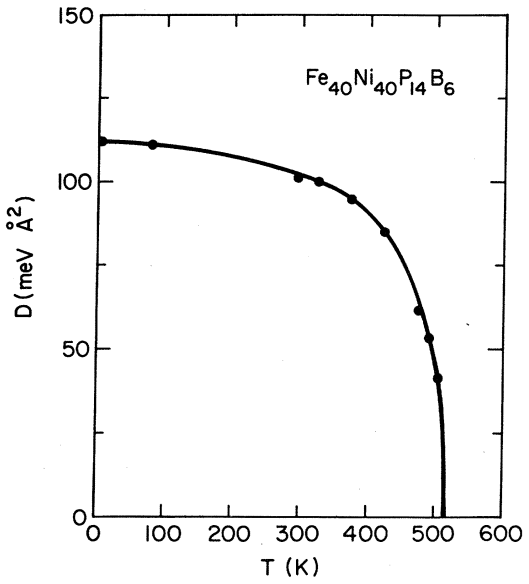

FIG. 5. Temperature dependence of the spin-wave-stiffness constant.

conventional unpolarized-beam triple-axis spectrometer. Details of these measurements will be given elsewhere; for the present purposes we simply remark that for $T<T_c$ ($T_c=513$ K), the spin-wave spectrum fits Eq. (2) to an excellent approximation as shown in Fig. 4. These data were taken at room temperature with a fixed incident energy of 13.7 meV, pyrolytic graphite monochromator, analyzer and filter, and 12′ FWHM collimators before and after the monochromator and analyzer. The observed peaks for neutron energy gain ($E<0$) and loss ($E>0$) are due to the destruction and creation of magnons, respectively. The elastic peak originates from nuclear scattering from the sample and furnace. The solid curves are a least-squares fit to a sum of three Gaussians, with the position of the central Gaussian fixed at $E=0$ and the width fixed to the measured energy resolution of 0.33 meV. The observed widths of the spin waves are solely instrumental in origin at these low temperatures. Note that at small values of Q the data cannot be extended to larger energy transfers due to the restrictions imposed by conservation of energy and momentum.

The spin-wave energies are also shown in Fig. 4 as a function of the square of the wave vector. The open circles give the peak positions for energy gain and the open squares give the peak positions for energy loss. The statistical accuracies for these data are smaller than the size of the points. There are significant corrections due to the effects of finite instrumental resolution, and the corrected data are shown by the triangles. These data are seen to obey Eq. (2) very well. The solid curve is a least-squares fit to a straight line, which yields a slope of (97 ± 3) meV Å^2 at room temperature.

The stiffness coefficient D obtained from such data is shown in Fig. 5 as a function of temperature. The renormalization of the spin-wave dispersion relation is typical of isotropic ferromagnetic systems. Note that at room temperature D has attained 83% of the saturated low-temperature value. Thus we do not expect much change in the dynamic susceptibility in going from room temperature to low temperatures; the primary effect for the observed scattering will be due to the change in the thermal population of the magnetic excitations of the system.

For convenience in referring to the time-of-flight data to be presented shortly, Fig. 6 shows a portion of the scattering function $S(Q)$. These data were taken with the spectrometer set for the elastic-scattering position. The wave-vector resolution is about the width of a point. The first peak in the structure factor occurs at $Q_0=3.08$ Å^{-1}.

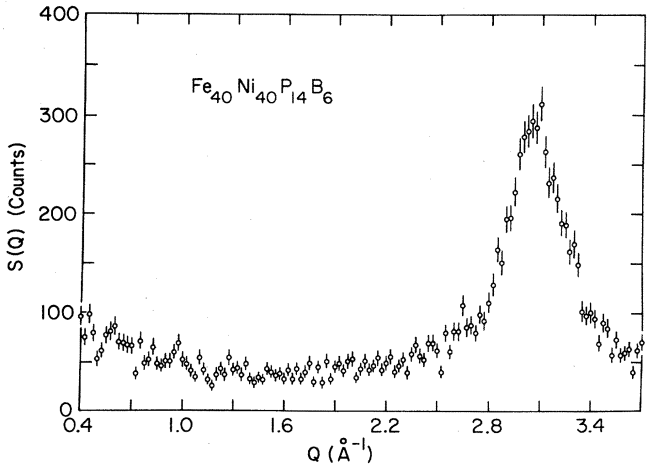

FIG. 6. Measurement of $S(Q)$ made with a triple-axis spectrometer set for elastic scattering.

For the measurements on the time-of-flight spectrometer, the sample was wound on a thin single crystal of silicon. The silicon contributed no measurable scattering in the region of interest and hence served as a very effective sample holder. The resulting sample was $3\times5\times0.5$ cm^3 and was used in symmetric transmission. The sample was checked on a three-axis polarized-beam spectrometer, and only small beam depolarization was found for the applied field of 5 kG used in the experiments. The sample had a neutron transmission of about 80% at 50 meV. Some absorption was present in the sample because of the natural boron which has a high neutron absorption coefficient; however, some absorption is helpful in that it reduces multiple scattering in the sample by not allowing the neutron to traverse along the sample and scatter again after the primary scattering. Multiple scattering undoubtedly gives some small extra intensity in the neutron scattering patterns. We have neglected this effect compared to the much stronger primary scattering.

Time-of-flight measurements were made on the amorphous sample $Fe_{40}Ni_{40}P_{14}B_6$ and the data reduced in the same manner as for the polycrystalline ferrite. Thirteen detector banks were used at scattering angles varying from 10.50° to 56.30°. E_0 was first chosen to be 49.71 meV to cover the energy-transfer range up to about 25 meV. Figure 7 shows $S(Q,E)$ and $\chi(Q,E)$ for some of the individual detectors. The trajectories of the scans in (Q,E) space are shown in Fig. 8. Note that the scans are almost constant-Q scans over the energy range of interest. Detectors 1–4 showed little inelastic scattering, and showed only the polarization-effect scattering near $E=0$. The width of the polarization-effect peak is again equal to the instrumental resolution of 4.5 meV. This suggests our data are subject to errors below ~9 meV, which is two resolution elements. Detector 5 shows the polarization-effect peak as well as the inelastic scattering intensity at the higher-energy transfers. Detector 8 is at a Q value near 3 Å^{-1}, which is near the Q value of the first peak of $S(Q)$. As with the powder, very strong, negative polarization-effect scattering is observed so that $S(Q,E)$ crosses $E=0$ at 4 meV. By the time 9 meV is reached, $S(Q,E)$ and $\chi(Q,E)$ are both large, but they drop off again at high energies unlike the pattern for the polycrystalline material.

A contour map of $\chi(Q,E)$ for all the detectors is shown in Fig. 8. Clearly we have strong scattering at energies where $S(Q)$ peaks. At the lowest energies the scattering drops off in intensity near $E=0$. However, we know that this is a resolution effect and that our data are not reliable much below the $2R$ point shown in the figure. At Q_0 the susceptibility as a function of energy shows a peak at ~12 meV, unlike the case of the polycrystal. This scattering then represents the "magnetic rotons" of the system in analogy with ^{4}He, although as we said earlier the analogy in many respects is not a good one. One might argue that the observed peak is not an intrinsic effect but is produced by resolution effects. However, our higher-resolution

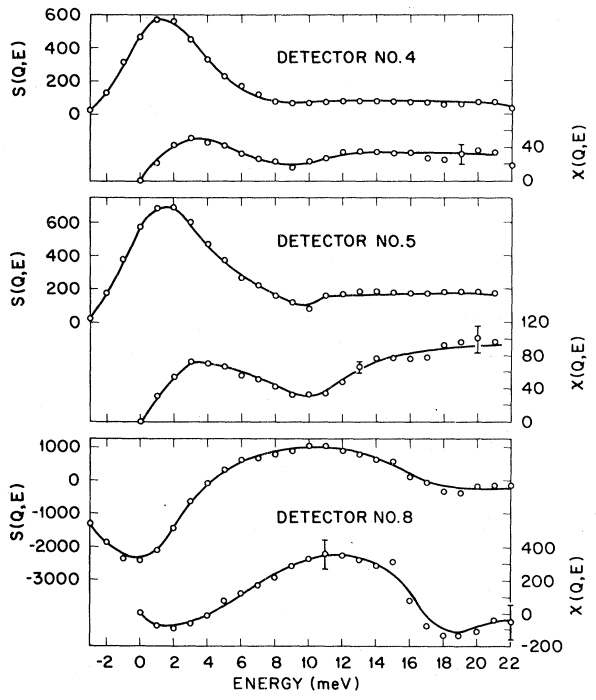

FIG. 7. Observed scattering $S(Q,E)$ at room temperature, and dynamic susceptibility $\chi(Q,E)$ for amorphous $Fe_{40}Ni_{40}P_{14}B_6$. The trajectories of the detectors in (Q,E) space are shown in Fig. 8. The incident energy employed was 49.7 meV. Detector 8 is at Q_0 and shows a clear peak in the scattering and the susceptibility. The scattering at high energies decreases considerably more rapidly than expected based on the umklapp model of a polycrystal.

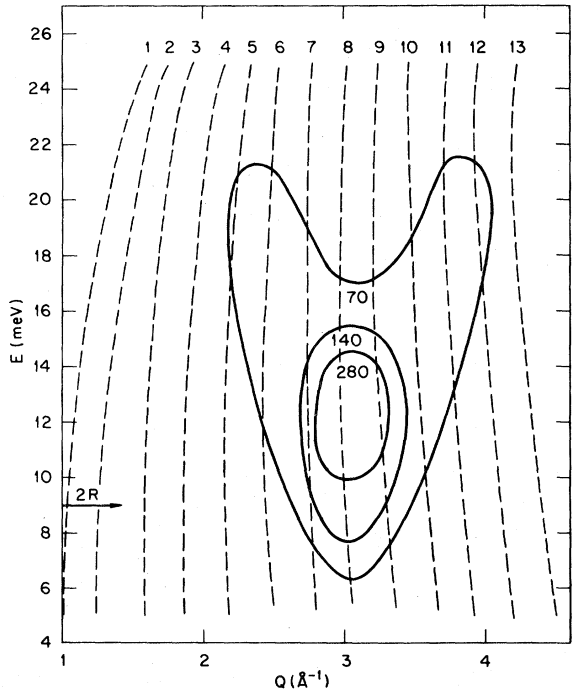

FIG. 8. Contour plot of the dynamic susceptibility for $Fe_{40}Ni_{40}P_{14}B_4$. The (Q,E) trajectories for the various detectors are shown by the dashed curves. The susceptibility shows a peak at Q_0 for $E\sim12$ meV, and then rapidly decreases at higher energies.

measurements presented below indicate that this is not the case.

The calculation of Shirane *et al.*[8] for an amorphous material consists of convoluting the polycrystalline spin waves with the structure factor $S(Q)$ so that the scattering is spread out in Q and is no longer a constant in the interior of a cone. As a function of Q the calculated scattering has a maximum at the peak in the structure factor $S(Q)$. The model is exact[16] in the limit of small ω and indeed is in agreement with experiment at low energies.[8] At higher energies our observed intensity has a minimum at Q_0. This effect appears to be intrinsic to the amorphous material and shows a clear difference between the umklapp model and our measurements at higher energies. Of course, at sufficiently high energies the overall density of magnetic states must decrease, but this is expected to occur above the present energy region of measurement for a material with a D of 100 meV Å^{-2}. A decrease in intensity at high energies near the peak at $S(Q)$ is observed in the one-dimensional calculations for disordered materials by Hall and Faulkner.[17] It is not clear, however, whether that structure would persist for three dimensions. Alben's[6] calculations do not seem sufficiently accurate to elucidate this point. Calculations by Singh and Roth[18] also show structure that has similarities to our experimental results but again only qualitative comparisons can be made. It would be valuable if higher-accuracy model calculations could be carried out. However, since our sample is metallic, the Heisenberg-type Hamiltonian used in the model calculations may not be applicable, especially in the higher-energy ranges where single-particle (Stoner) excitations may affect the intensities of the magnetic excitations.

To learn anything about the lower-energy part of the spectrum measurements have to be made with higher resolution. We thus made measurements with an incident energy of 37.79 meV. Detectors were placed at angles ranging from 23° to 65° to cover the Q range of interest. Since the Q scale is expanded somewhat in angle with this smaller incident energy, we improved the statistical accuracy of our data by adding detectors in pairs. Figure 9 shows data taken at the lower incoming energy. For detectors 1 and 2, which are at a Q of about 1.8 Å^{-1}, we see the usual polarization effect near $E=0$ but not much inelastic scattering away from $E=0$. The trajectories of the scans in (Q,E) space are shown in Fig. 10. The lower half of Fig. 9 shows the result obtained from detectors 6 and 7, which were located to measure a Q near the peak in $S(Q)$. Again we see large negative scattering near $E=0$ resulting from polarization effects. Two resolution elements are about 6 meV for the incoming energy used, so our data should be reliable for energies larger than this. We see that $\chi(Q,E)$ continues to rise well above 6 meV, reaching a maximum near 12 meV. Of course, $\chi(Q,E)$ must peak away from zero (as for detectors 1 and 2) since $\chi(Q,E)=0$ for $E=0$. Thus, a peak in $\chi(Q,E)$ neither implies a peak in $S(Q,E)$, depending on the instrumental resolution and measuring temperature, nor does it imply that there is any gap in the spectrum near $E=0$. Shirane *et al.*[8] have made high-resolution measurements on other amorphous systems near $E=0$ and found that

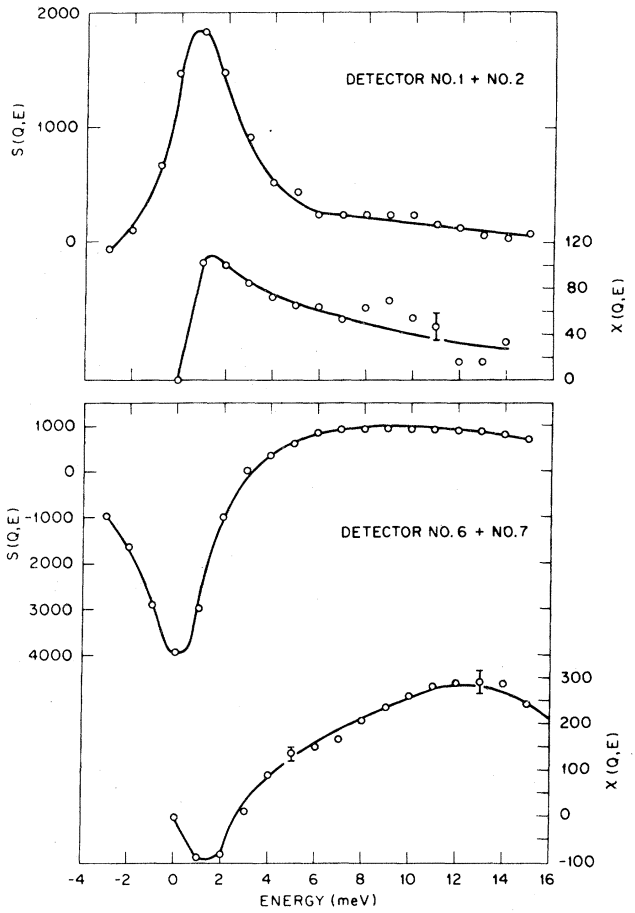

FIG. 9. Higher-resolution data for $Fe_{40}Ni_{40}P_{14}B_4$ taken with an incident energy of 37.79 meV. The (Q,E) trajectories are shown in the contour plot (Fig. 10). Detectors 6 and 7 are at Q_0. Note that the susceptibility shows a peak at ~ 12 meV, as do the coarser resolution data of Figs. 7 and 8.

for room temperature, $S(Q,E)$ appears largest near $E=0$. As the resolution was improved, $S(Q,E)$ could be measured to lower energies. We agree with these measurements. We also feel that no evidence exists to suggest that any gap exists in the magnetic excitations in any amorphous material measured so far, including Co_4P and $Fe_{75}P_{15}C_{10}$, and that excitations extend to low energies in these materials. Use of the word gap resulted[4,5] from comparison to ^{4}He where a true gap exists, and the word gap is really improper for amorphous materials. The time-of-flight measurements, however, show that $\chi(Q,E)$ has a maximum near $E=12$ meV for $Fe_{40}Ni_{40}P_{14}B_6$, which is different from the result expected for a polycrystalline or umklapp model. We believe that this maximum is intrinsic to these amorphous systems and is not a spurious effect caused by instrumental resolution. Thus the correct statement is that at Q_0 there appears to be a maximum at finite energy in the density of magnetic states.

Figure 10 shows a contour map of $\chi(Q,E)$, where a maximum in the scattering is found well above the two-resolution element value of 6 meV. We would like stronger evidence for the peak in $\chi(Q,E)$, as it may be that

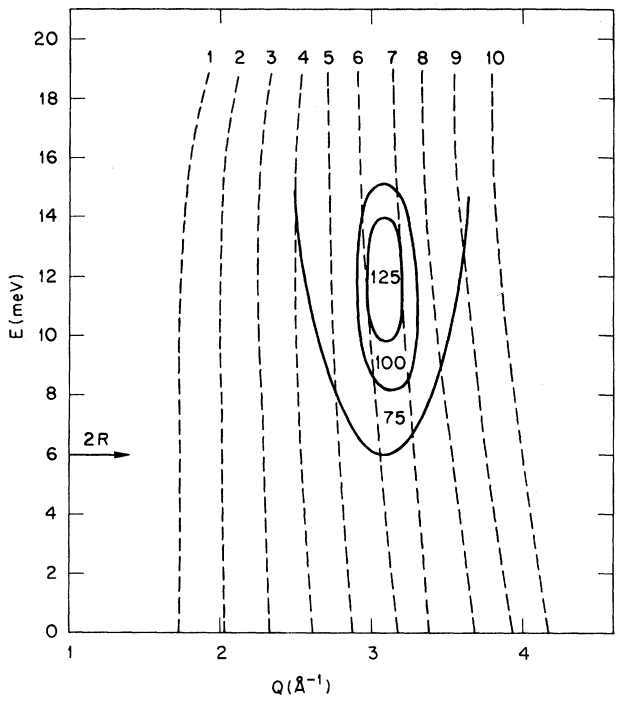

FIG. 10. Contour plot of $\chi(Q,E)$ obtained from the higher-resolution data taken on $Fe_{40}Ni_{40}P_{16}B_4$. The dashed curves signify the (Q,E) trajectories of the detectors. The intensity contours correspond to the counts in a single detector.

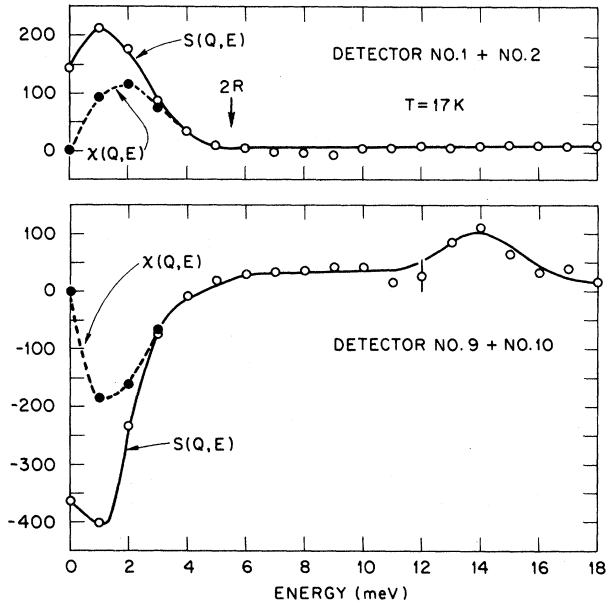

FIG. 11. Data for $Fe_{40}Ni_{40}P_{16}B_4$ taken at low temperatures (17 K) so that $S(Q,E)$ and $\chi(Q,E)$ are indistinguishable for $E>4$ meV. The data in adjacent detectors have been added to increase the statistical accuracy. Detectors 9 and 10 are for $Q\sim Q_0$, and a peak is seen at $E\sim 14$ meV.

one must go beyond two-resolution elements to get proper data, although this seemed sufficient for the polycrystal. We would need a lower incident energy for us to obtain much better resolution, which would move the scattering pattern out in angle such that the region of interest would be unreachable because of the limits placed on the scattering angle by the electromagnet that provides the sample's field. More experiments to elucidate this point would be welcome.

An additional measurement that we made was to measure the scattering at low temperatures. At $T=0$, $\chi(Q,E)=S(Q,E)$, so that we only have to deal with one function and interpretation of the results is simplified. There is no evidence that $S(Q,E)$ has a peak at a finite energy at room temperature; however, at low temperatures, as $S(Q,E)$ becomes increasingly similar to $\chi(Q,E)$, a finite-energy peak may develop. Low-temperature measurements further insure the establishment of fundamental ground-state properties. Our sample was placed in a low-temperature closed-cycle refrigerator that could be placed between the magnet-pole tips. The sample was field-cooled to 17 K, which was the lowest temperature the refrigerator could attain. Since aluminum heat shields were used, the measurement was hampered by Al powder lines that lie in the Q region of interest. The experimental conditions were identical to those used in the higher-resolution measurements with an incident energy of 37.79 meV. The detector positions were different as they had been moved to lower angles for a polycrystalline measurement so that the Q's sampled by each of the detectors were different. However, this does not change the measurement in any way as each detector's efficiency was calibrated against a standard vanadium sample before each measurement.

Results of the measurements are shown in Fig. 11. Because the temperature is low, $S(Q,E)$ and $\chi(Q,E)$ differ from each other only at low energies and become indistinguishable for $E>4$ meV. Again, detectors were added in pairs for increased accuracy. Detectors 1 and 2 were at a Q value of about 1.4 Å^{-1} and showed nothing but the usual polarization effect near $E=0$. Detectors 9 and 10 were centered at about 3.3 Å^{-1} for $E=0$, which mostly avoids the (200) Al powder line at 3.10 Å^{-1}. The trajectory in (E,Q) space is at a little lower Q than for detector 7 of Fig. 10. The (E,Q) trajectory crosses the region of interest, which is between 5 and 15 mV and near 3.14 Å^{-1}. The scattering from the Al heat shields of the low-temperature refrigerator made measurements difficult in the Q region where there were Al powder lines. A contour plot of the low-temperature measurements could not be constructed. Again, we see the negative effective scattering near $E=0$. This scattering is smaller now, because T is small. Above two-resolution elements, or at about 6 meV, the scattering is quite flat except for a peak in the region near 14 meV, close to where the maximum in the scattering pattern was observed at room temperature. For low temperatures then, $S(Q,E)$ [which is identical to $\chi(Q,E)$] appears to have a maximum in the scattering intensity at an energy removed from $E=0$. This result is not expected for a model of an amorphous magnet based on a polycrystal. Higher-resolution measurements at lower temperatures would be helpful in elucidating this point.

DISCUSSION AND CONCLUSIONS

New measurements made on a large sample of $Fe_{40}N_{14}P_{14}B_6$ show that there are low-lying magnetic excitations near the first peak in the static structure factor $S(Q)$, in agreement with observations made on other amorphous systems. Unfortunately, it is difficult to calculate the excitations in realistic models of an amorphous material sufficiently accurately to obtain a good comparison with our measurements. Hopefully, better calculations will be available in the future.

Our measurements are consistent with those of Shirane *et al.*,[8] and we are in agreement that excitations exist near $E=0$ at the Q position for the maximum in $S(Q)$. Their higher-resolution measurements have provided information at lower energies and established that no gap exists in the excitation spectrum for energies as small as 2 meV. We further agree that no reliable measurements are possible once the magnetic excitation energy becomes smaller than the instrumental width.

Our measurements at higher energies depart from expectations based on the umklapp model. Of course, one would not expect this model to give exact results at all energies for an amorphous material, as it employs a number of approximations which at some level of refinement of the measurement will become apparent. We observe two differences in particular. First, at high energies the scattering at the Q corresponding to the peak in $S(Q)$ falls off faster with energy than at Q's slightly removed from this value. Thus at higher energies the scattering as a function of Q displays maxima on either side of Q_0. A similar effect was observed in the earlier measurements. The second effect is more difficult to substantiate but is strongly suggested by our data; that $\chi(Q,E)$ at Q_0 peaks at an energy well removed from $E=0$. We would expect $S(Q,E)$ measured near $T=0$ to do likewise, and indeed our low-temperature measurements show a peak in $S(Q_0,E)$. For $Fe_{40}Ni_{40}P_{15}B_6$ this value of energy is about 12 meV, which is a more convenient energy to observe than in the other materials studied so far. We would welcome additional measurements to help resolve this point, and feel that higher-resolution low-temperature measurements would be particularly useful.

The measurements of Paul *et al.*[9] were made with quite coarse energy resolutions of about 15 and 25 meV FWHM, and thus the criterion of being two-resolution elements removed from $E=0$ suggests that the data are distorted by resolution and depolarization effects up to quite high energies. Nevertheless, the overall results agree in most respects with the data we report here, within the limits of comparisons of these difficult experiments.

ACKNOWLEDGMENTS

We would like to thank G. Shirane and J. D. Axe for helpful discussions. The spin-flip pulser used in the experiment was built at Ford Scientific Research Laboratory and made available to us by S. A. Werner. Research at Oak Ridge National Laboratory was sponsored by the Division of Materials Sciences, U. S. Department of Energy, under Contract No. W-7405-Eng-26 with the Union Carbide Corporation. Work at Maryland was supported by the National Science Foundation, Department of Materials Research, under Contract No. DMR82-07958.

---

[1] A number of experiments have shown that long-wavelength spin waves can be measured by neutron scattering in metallic glasses. The first measurements were made by J. D. Axe, L. Passell, and C. C. Tsuei, in *Magnetism and Magnetic Materials—1974 (San Francisco)*, Proceedings of the 20th Annual Conference on Magnetism and Magnetic Materials, edited by C. D. Graham, G. H. Lander, and J. J. Rhyne (AIP, New York, 1975), p. 119; H. A. Mook, D. Pan, J. D. Axe, and L. Passell, *ibid.*, p. 112.

[2] See, for example, J. W. Lynn, G. Shirane, and R. J. Birgeneau, in *Magnetism and Magnetic Materials—1976 (Joint MMM-Intermag Conference, Pittsburgh)*, Partial Proceedings of the First Joint MMM-Intermag Conference, edited by J. J. Becker and G. H. Lander (AIP, New York, 1976), p. 313; J. D. Axe, G. Shirane, T. Mizoguchi, and K. Yamauchi, Phys. Rev. B 15, 2763 (1977); R. J. Birgeneau, J. A. Tarvin, G. Shirane, E. N. Gyorgy, R. C. Sherwood, H. S. Chen, and C. L. Chien, *ibid.* 18, 2192 (1978); J. J. Rhyne, J. W. Lynn, F. E. Luborsky, and J. L. Walter, J. Appl. Phys. 50, 1583 (1979), and references therein.

[3] H. A. Mook, N. Wakabayashi, and D. Pan, Phys. Rev. Lett. 34, 1029 (1975).

[4] H. A. Mook and C. C. Tsuei, Phys. Rev. B 16, 2184 (1977).

[5] H. A. Mook, J. Appl. Phys. 49, 1665 (1978).

[6] R. Alben, in *Magnetism and Magnetic Materials—1975 (Philadelphia)*, Proceedings of the 21st Annual Conference on Magnetism and Magnetic Materials, edited by J. J. Becker, G. H. Lander, and J. J. Rhyne (AIP, New York, 1976), p. 136.

[7] A recent review is given by H. S. Chen, Rep. Prog. Phys. 43, 353 (1980).

[8] G. Shirane, J. D. Axe, C. F. Majkrzak, and T. Mizoguchi, Phys. Rev. B 26, 2575 (1982).

[9] D. M. K. Paul, R. A. Cowley, W. G. Stirling, N. Cowlam, and H. A. Davies, J. Phys. F 12, 2687 (1982).

[10] For temperatures near (and above) T_c, $S^{-+}(Q,E)$ becomes appreciable for $E>0$ as small clusters of correlated spins begin to deviate from the nominal z axis. For temperatures well below T_c, however, this effect can be neglected. See, for example, R. D. Lowde, R. M. Moon, B. Pagonis, C. H. Perry, J. B. Sokoloff, R. S. Vaughan-Watkins, M. C. K. Wiltshire, and J. Crangle, J. Phys. F 13, 249 (1983); O. A. Pringle and H. A. Mook (unpublished).

[11] R. M. Nicklow, N. C. Koon, C. M. Williams, and J. B. Milstein, Phys. Rev. Lett. 36, 532 (1976).

[12] W. Marshall and S. W. Lovesey, *Theory of Thermal Neutron Scattering* (Oxford University Press, London, 1971), Chap. 8.

[13] H. A. Alperin, O. Steinsvoll, R. Nathans, and G. Shirane, Phys. Rev. 154, 508 (1967).

[14] V. C. Rakhecha, L. Madhav Rao, N. S. Satya Murthy, and B. S. Srinivasan, Phys. Lett. 40A, 101 (1972).

[15] F. Keffer, *Encyclopedia of Physics* (Springer, Berlin, 1966), Vol. XVIII, p. 49.

[16] G. Shirane and J. D. Axe (private communication).

[17] D. G. Hall and J. S. Faulkner, Phys. Rev. B 15, 5850 (1979).

[18] V. A. Singh and L. M. Roth, J. Appl. Phys. 49, 1642 (1978).